ELSEVIER

CrossMark

Available online at www.sciencedirect.com

ScienceDirect

Procedia Engineering 140 (2016) 107 – 114

Procedia Engineering

www.elsevier.com/locate/procedia

MRS Singapore – ICMAT Symposia Proceedings

8th International Conference on Materials for Advanced Technologies

Photonic integrated circuits based on quantum well intermixing techniques

Lianping Hou*, John H. Marsh

School of Engnieering, University of Glasgow, Glasgow, G12 8LT ,UK

Abstract

The passive sections of a monolithic device must have a wider bandgap than the active regions to reduce losses due to direct interband absorption. Such bandgap engineering is usually realized by complicated regrown butt-joint or selective-area growth techniques. We, however, have developed a simple, flexible and low-cost alternative technique – quantum well intermixing (QWI) – to increase the bandgap in selected areas of an integrated device post-growth. To verify the QWI process, we have fabricated the following demonstrators: a 40 GHz semiconductor mode-locked laser producing pulses as short as 490 fs; a 10 GHz passively mode-locked extended cavity laser integrated with surface-etched distributed Bragg reflector (DBR) which can be tuned in both wavelength and pulse repetition rate; four 10 GHz 1.55 μm AlGaInAs/InP mode-locked surfaced-etched DBR lasers integrated combiner, a semiconductor optical amplifier and modulator where the four channels can be operated separately or simultaneously; a CWDM source with 12 nm wavelength separation based on an AlGaInAs/InP integrated distributed feedback laser array; and a 1.55 μm DFB laser monolithically integrated with power amplifier array. In all these applications, QWI has the advantage of eliminating crystal regrowth and the associated stringent tolerance requirements that are required in traditional integration schemes.

Crown Copyright © 2016 Published by Elsevier Ltd. This is an open access article under the CC BY-NC-ND license (http://creativecommons.org/licenses/by-nc-nd/4.0/).
Selection and/or peer-review under responsibility of the scientific committee of Symposium 2015 ICMAT

Keywords: Photonic integrated circuits; quantum well interxming

* Corresponding author. Tel.: +44-(0)141-330-6008; fax: +44-(0)141-330-4885.
E-mail address: Lianping.hou@glasgow.ac.uk

1877-7058 Crown Copyright © 2016 Published by Elsevier Ltd. This is an open access article under the CC BY-NC-ND license (http://creativecommons.org/licenses/by-nc-nd/4.0/).
Selection and/or peer-review under responsibility of the scientific committee of Symposium 2015 ICMAT
doi:10.1016/j.proeng.2015.10.152

1. Introduction

Photonic integrated circuits (PICs) are the key for realizing multifunctional and low-cost devices for optical communications and for other miniature and portable optical systems. Such applications include coarse wavelength division multiplexing (CWMD) and dense wavelength division multiplexing (DWDM) systems. Several technologies based on epitaxy have been developed to realize the integration of devices with different bandgap wavelengths, such as butt-joint regrowth (BJR), selective area growth (SAG), and asymmetric twin waveguide (ATG) designs. The big challenge for BJR is to control the etching and regrowth sufficiently precisely, to avoid defect generation during regrowth and to obtain a high quality butt-joint interface with low scattering loss. SAG technology is useful in simultaneously fabricating active devices with different bandgap energies, however it is not suitable for the integration of active and passive devices. The ATG technique needs multiple steps of material etching with accurate control, especially for etching active tapers, and there is an inevitable transmission loss from active to passive waveguides. ATG cannot meet the flexibility necessary for large-scale photonic integration due to its limited number of bandgaps. Compared with conventional techniques for photonic integration based on selective etching and re-growth, post-growth processing based on quantum-well intermixing (QWI) offers a simple, flexible and low-cost alternative [1].

Several QWI techniques have been proposed and demonstrated, including impurity induced disordering (IID) [2], photo-absorption-induced disordering (PAID) [3], pulsed-PAID (P-PAID) [4] and impurity-free vacancy-enhanced disordering (IFVD) [5]. For IID, relatively high concentrations (10^{18} cm^{-3}) of active dopants are typically required, giving rise to significant free-carrier absorption (>10 cm^{-1}) in bandgap widened waveguides. If high energy ion implantation is used, lattice damage may degrade the material quality. PAID has the problem of poor spatial definition. P-PAID uses ultra-short laser pulses to break lattice bonds and the intensity variation across the laser Gaussian beam results in non-uniform intermixing.

In this paper, we have used a universal QWI process based on a sputtered SiO_2 film. Bandgap shifts as large as 100 nm are obtained at a very low rapid thermal annealing (RTA) temperature (660 °C). Based on this simple and reliable QWI technique, we report here several PIC devices which have high quality performance and wide application particularly in optical communications systems.

2. Wafer structure and universal QWI process

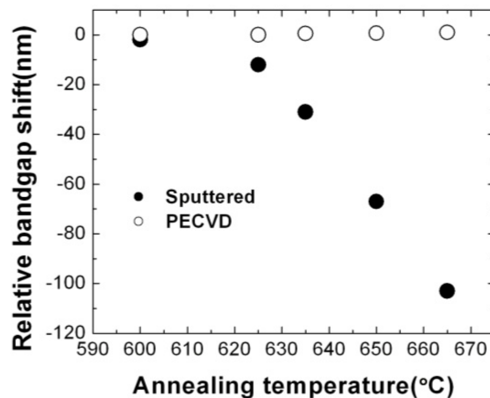

Fig.1. Relative bandgap shift versus annealing temperature for samples covered with sputtered and PECVD SiO_2 after 60 s of RTA process.

The samples used in the experiment were based on commercial AlGaInAs 1550 nm laser diode (LD) wafers [6], with an active region consisting of five quantum wells (QWs) (6 nm thick QWs separated by 10 nm thick barriers), where both wells and barriers were Al-quaternary based. Compressive strain of the active region materials (1.2% in the QWs and -0.5% in the barriers) ensured that the radiative transitions were predominantly TE polarized. Compared with the InGaAsP material system, the saturable absorption recovery time based on AlGaInAs/InP material is much faster which makes it especially suitable for the fabrication of semiconductor mode-locked lasers (SMLLs) [7].

A 200-nm-thick sputtered SiO_2 film was selectively deposited on the passive waveguide areas, and then the whole wafer was covered with a protective 200-nm-thick plasma-enhanced chemical vapor deposition (PECVD) SiO_2 film. The sample was subsequently annealed at 660 °C for 60 s leading to a targeted bandgap shift of 100 nm for the passive section only. The active sections did not exhibit any significant shift at the same RTA temperature, as shown in Fig.1. The QWI mechanism and process for the universal QWI technique have been described in [8, 9].

3. Application of universal QWI for the PIC devices

3.1. 10-GHz mode-locked extended cavity laser integrated with surface-etch distributed Bragg reflector

Monolithic mode-locked semiconductor lasers are commercially attractive with respect to compactness, ease of handling, robustness, performance stability, power consumption, and cost savings. Distributed Bragg reflectors (DBRs) are indispensable for controlling the spectral bandwidth, the center wavelength, while additionally providing tuning possibilities of the pulse repetition rate [10].In comparison with the traditional approach of buried-gratings, lasers shown in this paper have advantages related to the use of surface-etched DBRs [11].

The 10-GHz monolithic integrated mode-locked DBR laser is shown in Fig. 2(a). The fabrication process used for the device and its dimensions are described in [12].

Fig. 2 also summarizes the dependence of the peak wavelength (W_p), pulse repetition frequency (F_r), pulse width and time bandwidth product (TBP) on the DBR tuning current, where the total injection currents to the gain section were fixed at 220, 240, and 260 mA, with V_{SA} = -3.0 V. For all investigated I_{gain} values, the peak wavelength initially experienced a quasi-continuous blue-shift when the I_{DBR} was increased from 0 mA to 11 mA, due band-filling (see Fig. 2(b)). At higher DBR currents, the peak wavelength remained constant. The discrete wavelength shifts are a result of the limited measurement resolution (0.06 nm resolution bandwidth) of the optical spectrum analyser (OSA).

From Fig. 2(c), we note typical trends, i.e. for all investigated V_{SA} and for a fixed I_{gain}, F_r decreases with increasing I_{DBR}. A tuning range of about 18 MHz was obtained when I_{DBR} was varied from 0 mA to 20 mA with I_{gain}= 260 mA. The frequency reduction with increasing I_{DBR} was consistent with the increase in the effective length due to lower absorption loss [13]. On the other hand, for a fixed value of I_{DBR} and V_{SA}, F_r decreased with increasing I_{gain}. These anomalously high frequency shifts are mainly caused by the detuning of the cavity roundtrip frequency by gain/absorber saturation effects [14]. A tuning range of about 36 MHz was obtained when I_{gain} was varied from 220 mA to 260 mA for I_{DBR} = 0 mA.

Fig. 2(d) shows the pulse width and TBP as a function of I_{DBR} at various values of I_{gain}. It is known that, for a fixed I_{DBR}, as I_{gain} is increased the optical intensity and unsaturated gain increase. Consequently, the gain saturation increases and the pulse width broadens, as shown in Fig. 2(d), due to chirp induced by self-phase modulation (SPM) [15]. For all applied I_{gain}, as I_{DBR} increased, the TBP initially reduced and then stabilized at around 0.6 when I_{DBR} reached 20 mA, which is somewhat larger than the transform-limited value (0.315 for $sech^2$ shape pulse). This is believed to be due to spectral broadening caused by SPM, mainly in the gain section [15].

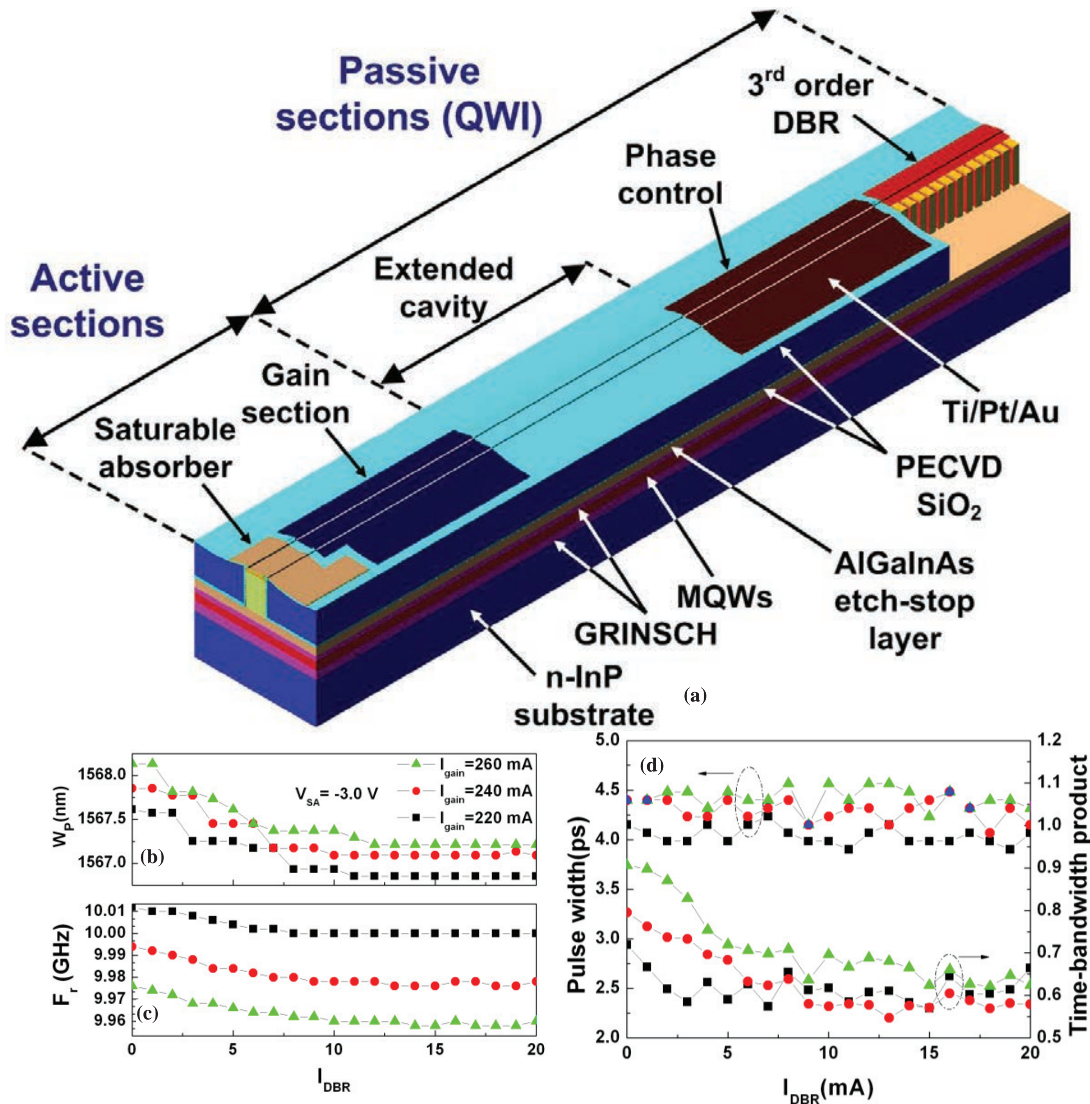

Fig. 2. (a) Schematic of the10 GHz extended cavity laser integrated with surface-etched DBR and (b) emission peak wavelength (W_P), (c) pulse repetition frequency (F_r), and (d) pulse width and TBPs vs. I_{DBR} for I_{gain} = 220, 240, and 260 mA while V_{SA} = -3.0 V and phase section left floating.

3.2. 10 GHz mode-locked laser array monolithically integrated with SOA and electro-absorption modulator

Based on the device described in Section 3.1, we extended the surface-etched DBR and QWI techniques to the fabrication of four 10 GHz 1.55-μm AlGaInAs/InP mode-locked surface-etched DBR lasers with a monolithically integrated 4×1 multimode-interference (MMI) optical combiner, a curved waveguide semiconductor optical amplifier (SOA) and electroabsorption modulator (EAM). The period of the DBR was varied from 734 nm to 740 nm from channel 1(CH1) to channel 4(CH4), respectively. An optical microscope picture of the overall laser array is shown in Fig. 3(a). The device dimensions and fabrication processes are described in [16].

Simultaneous CW lasing spectra (RBW=0.06 nm) of the four MLDLDs from the same array are show in Fig. 3(b) under the free running conditions stated in the caption of Fig. 3(b). The spacing of the spectra was about 5 nm. The -

3 dB bandwidth was within 0.8-1.3 nm. Fig. 3(c) shows the corresponding RF signals, which confirmed that the four channels can be operated either simultaneously, with four corresponding pulse repetition frequencies, F_r, or individually, enabling the selection of a single F_r. The corresponding autocorrelation trace has a small pedestal and some amplitude modulation. This is due to the different F_r of the four channels. Varying the I_{DBR}, I_{phase}, I_{gain}, and V_{SA} enable F_r to be tuned at the cost of shifting the designated wavelength registration. However, due to the ~5 nm channel spacing, obtaining the same F_r is extremely difficult to achieve in practice when passively mode locking.

In order to overcome this, a simple synchronization approach was applied. Under the same operating condition as stated in Fig. 3(b), we used a 10 GHz active fiber mode locked laser (Pritel) as a seed, operating at the peak wavelength of 1550 nm and with a compressed pulse width of 0.73 ps, and this seed was injected into our device from the angled EAM side. It was found that when, the seed power was >10 dB, all 4-channels were synchronized at an F_r of 10 GHz. The pulse width was 3.14 ps, assuming a sech^2 shape, which is less than the free running value of 5.39 ps.

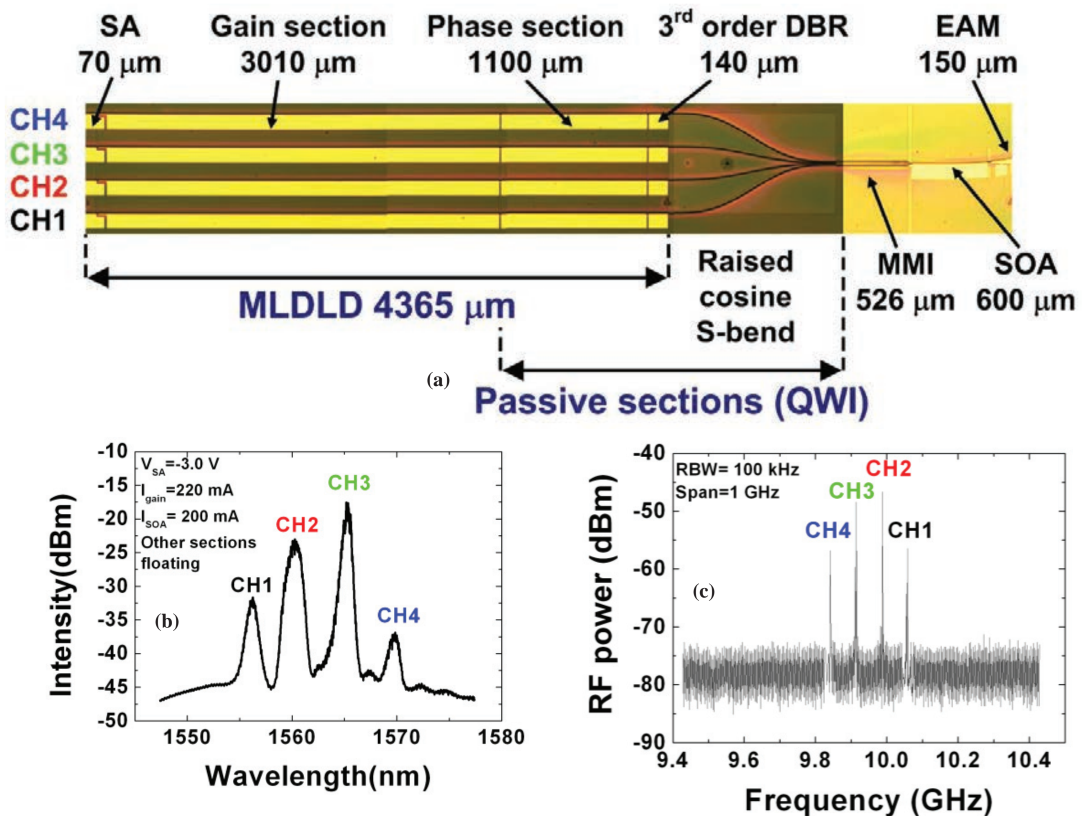

Fig.3. (a) Optical microscope picture of the overall laser array and (b) simultaneous lasing spectra of all four channels and (c) corresponding RF signals

3.3. Coherent beam combination laser diode

Here we report a simple, scalable monolithically integrated system comprising a laterally-coupled 1.55 μm distributed feedback (DFB) laser feeding two stages of MMI couplers and SOAs to deliver high power beams with a quasi-single-spatial-mode far field pattern (FFP) [17]. The schematic of the fabricated device along with its dimensions are shown in Fig. 4(a). Figs 4(b) and (c) show SEM pictures of the side wall grating of the DFB laser and the 1×2 MMI. These coherent beam combination (CBC) laser diodes offer the potential for increasing the brightness of the output beam while maintaining a narrow spectrum bandwidth, which has many applications such as Raman pumps for fiber communication systems, spectroscopy, remote sensing, free-space communications, eye-safe laser based radar (LIDAR), and wavelength conversion in nonlinear materials [18]. Fig. 4(d) shows the quasi-single spatial-mode FFP measured from the output facets of SOAs 3-6 using I_{DFB} = 60 mA, $I_{SOA1\text{-}SOA2}$ = 120 mA, with two (SOA5 and SOA6, black solid line), three (SOA4-SOA6, red dash line), and four (SOA3-SOA6, green dot line) output SOAs simultaneously pumped, each with an injection current of 120 mA. Furthermore, we used diffraction theory to simulate the FFP when all four output SOAs are driven (blue line), and the envelope is similar to that of the measured results. 1D optical beam steering could be achieved by controlling the phase across the SOA3-SOA6 array.

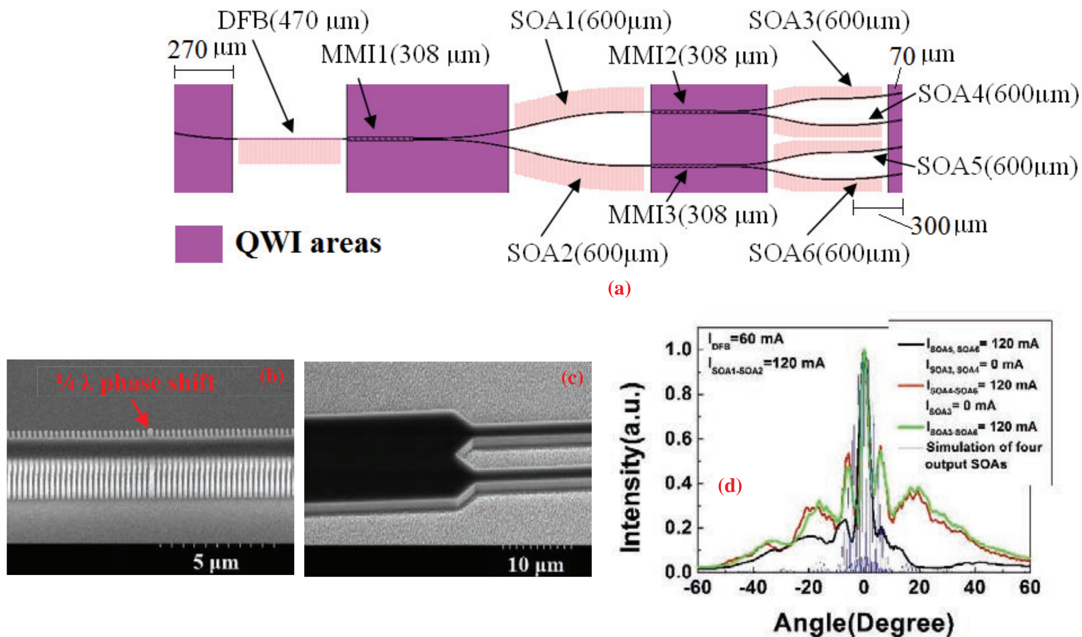

Fig. 4. (a) Schematic of CBC device, (b) SEM picture of the first-order 50% duty cycle sidewall gratings with a 0.6 μm recess and λ/4 phase shift, (c) the MMI output side , (d) measured in-plane FFP at I_{DFB} =60 mA, $I_{SOA1\text{-}SOA2}$ =120 mA, with two (black solid line), three (red line), four (green line) output SOAs pumped with an injection current of 120 mA and simulation (blue line) of four output SOAs using diffraction theory. Note the FFPs are offset by 32° because of the angled facet.

3.4. CWDM transmitter chip

Using QWI and sidewall grating techniques, we also realized the monolithic integration of four 1.50 μm range AlGaInAs/InP DFB lasers in a PIC for CWDM. In addition to the four DFB lasers, the PIC comprised a 4×1 MMI combiner, a curved SOA and an EAM as shown in Fig. 5(a)-(d) [19]. The four channels span the wavelength range from 1530 to 1566 nm with a channel spacing of nearly 12 nm and can operate separately or simultaneously which is suitable for CWDM transmitter chip (see Fig. 5(e)). Here we used a novel epitaxial structure consisting of a 3-QW active layer incorporating a passive far-field reduction layer (FRL) to produce a FFP at the output waveguide facet

which is as small as 21.2° × 25.1°. This feature results in a coupling efficiency to an angled-end single mode fiber of twice that of a conventional device design [20]. Due to the low internal loss (8/cm) and the longer cavity length of the DFB laser arrays, an optical linewidth of 64 kHz was achieved [21].

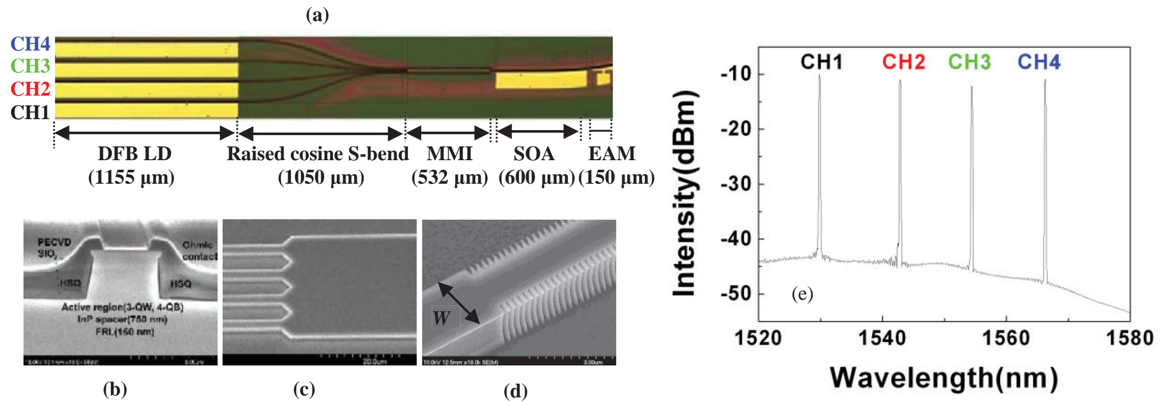

Fig. 5. (a) Optical microscope picture of the overall laser array, (b) scanning electron microscope (SEM) picture of a cross section of the ridge waveguide, (c) MMI, (d) uniform first-order sidewall gratings with a 50% duty cycle and 0.4 μm recess depth d, (e) Simultaneous lasing spectra of all four channels for I_{DFB} =150 mA, I_{SOA}=90 mA and EAM section left floating

3.5. Femtosecond pulse generation semiconductor mode-locked laser

Based on the novel wafer structure with 3 QWs and FRL described in Section 3.4, and using QWI to create a passive section within the laser cavity of a 40 GHz SMLL (Fig.6(a)), we can shorten the length of the gain section, reducing SPM effects and therefore suppressing the pulse broadening that takes place in the gain section. As a result, we achieved a dramatically shortened pulse width of 490 ps (Fig. 6(b)), which is, to the best of our knowledge, the shortest pulse obtained from any directly electrically pumped quantum well SMLL. The mode-locking range is relatively large and the ultra-narrow pulse width is very stable over a broad range of driving conditions [22].

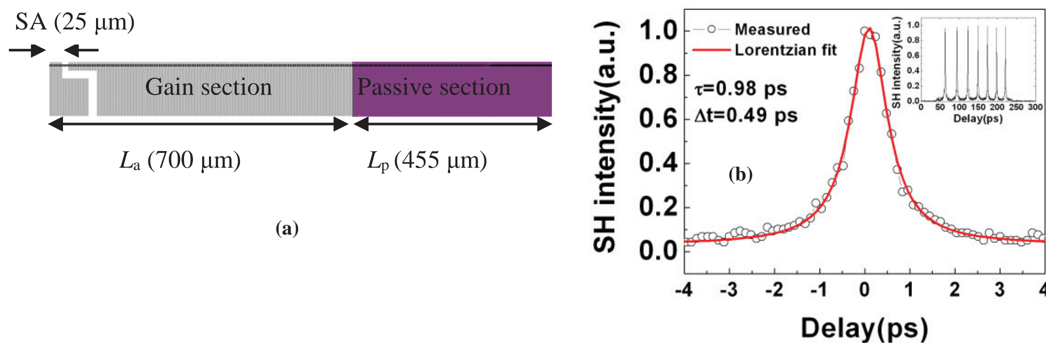

Fig. 6. Diagram of the extended cavity 40 GHz SMLL and the measured isolated pulse fitting by Lorentzian shape and measured autocorrelation pulse trains (inset)

4. Conclusion

Our QWI is performed post-growth and is a universal, simple, flexible and low-cost alternative technique to conventional complicated and time-consuming techniques, such as BJR, SAG, and ATG. Using the universal QWI technique, we have demonstrated here several PIC devices with applications in advanced communications systems. All of these PICs exhibit high performance, partly as a result of the very low optical reflections and scattering at the active-passive interfaces defined by QWI.

Acknowledgements

The authors would like to acknowledge the staff of the James Watt Nanofabrication Centre at the University of Glasgow for help in fabricating the devices reported in this paper. Some this work was supported by EPSRC under grant EP/E065112/1.

References

[1] J. H. Marsh, P. Cusamano, A. C. Bryce, B. S. Ooi, and S. G. Ayling, GaAs/AlGaAs photonic integrated circuits fabricated using impurity-free vacancy disordering, Proc. SPIE 2401 (1995) 74–85.
[2] W. D. Laidig, N. Holonyak, Jr., M. D. Camras, K. Hess, J. J. Coleman, P.D. Dapkus, and J. Bardeen, Disorder of an AlAs-GaAs superlattice by impurity diffusion, Appl. Phys. Lett. 38 (1981) 776–778.
[3] A. McKee, C. J. McLean, G. Lullo, A. C. Bryce, R. M. Rue, and J. H. Marsh, Monolithic integration in InGaAs-InGaAsP multiple-quantum-well structures using laser intermixing, IEEE J. Quantum Electron. 33 (1997) 45–55.
[4] J. H. Marsh, Laser induced quantum well intermixing for optoelectronic devices, LEOS 2(1996) 380–381.
[5] G. Deppe, L. J. Guido, N. Holonyak, K. C. Hseih, R. D. Burnham, L.Thornton, and T. L. Paoli, Stripe-geometry quantum well heterostructure $Al_xGa_{1-x}As$-GaAs lasers defined by defect diffusion, Appl. Phys. Lett. 49 (1986) 510 –512.
[6] L. Hou, P. Stolarz, J. Javaloyes, R. Green, C. Ironside, M. Sorel, and A. C. Bryce, Subpicosecond pulse generation at quasi-40-GHz using a passively mode locked AlGaInAs/InP 1.55 μm strained quantum well laser, IEEE Photon. Technol. Lett. 21(2009) 1731–1733.
[7] R. P. Green, M. Haji, L. Hou, G. Mezosi, R. Dylewicz and A. E. Kelly, Fast saturable absorption and 10 GHz wavelength conversion in Al-quaternary multiple quantum wells, Opt. Express 19 (2011) 9737–9743.
[8] O.P. Kowalski, C.J. Hamilton, S.D. McDougall, J.H. Marsh, A.C. Bryce, R. M. De La Rue, B. Vögele, C.R. Stanley, C.C. Button, J.S. Roberts, A universal damage induced technique for quantum well intermixing, Appl. Phys. Lett. 72 (1998) 581–583.
[9] L. Hou, M. Haji, R. Dylewicz, B. Qiu, A. C. Bryce, Monolithic 45-GHz Mode locked surface-etched DBR laser using quantum well intermixing technology, IEEE Photon. Technol. Lett. 22 (2010) 1039–1041.
[10] E. Zielinski, E. Lach, J. Bouayad-Amine, H. Haisch, E. Kuhn, M. Schilling, and J. Weber, Monolithic multisegment mode-locked DBR laser for wavelength tunable picosecond pulse generation, IEEE J. Select. Topics Quantum Electron. 3 (1997) 230–232.
[11] L. Hou, R. Dylewicz, M. Haji, P. Stolarz, B. Qiu, and A. C. Bryce, Monolithic 40 GHz passively mode-locked AlGaInAs/InP 1.55 μm MQW laser with surface-etched distributed Bragg reflector, IEEE Photon. Technol. Lett. 22 (2010) 1503–1505.
[12] L. Hou, M. Haji, R. Dylewicz, B.C. Qiu, A. Catrina Bryc, 10 GHz mode-locked extended cavity laser integrated with surface-etched DBR fabricated by Quantum Well Intermixing, IEEE Photon. Technol. Lett. 23 (2011) 82–84.
[13] I. Ogura, H. Kurita, T. Sasaki, and H. Yokoyama, Precise operation-frequency control of monolithic mode-locked laser diodes for high-speed optical communication and all-optical signal processing, Opt. Quantum Electron. 33 (2001) 709–725.
[14] S. Arahira and Y. Ogawa, Repetition–frequency tuning of monolithic passively mode-locked semiconductor lasers with integrated extended cavities, IEEE J. Quantum Electron. 33 (1997), 255–264.
[15] G. P. Agrawal and N. A. Olsson, Self-phase modulation and spectral broadening of optical pulses in semiconductor laser amplifiers, IEEE J. Quantum Electron. 25 (1989) 2297–2306.
[16] L. Hou, M. Haji, B.C. Qiu, A. Catrina. Bryce, Mode-locked laser array monolithically integrated with MMI combiner, SOA and EA modulator, IEEE Photon. Technol. Lett. 23(2011)1064–1066.
[17] L. Hou, J. H. Marsh, 1.55 μm DFB laser monolithically integrated with power amplifier array, Opt. Lett. 40(2015) 213–216.
[18] S. R. Selmic, G. A. Evans, T. M. Chou, J. B. Kirk, J. N. Walpole, J. P. Donnelly, C. T. Harris, and L. J. Missaggia, Single frequency 1550-nm AlGaInAs–InP tapered high-power laser with a distributed Bragg reflector, IEEE Photon. Technol. Lett. 14 (2002) 890–892.
[19] L. Hou, M. Haji, J. Akbar,J. H. Marsh, A. C. Bryce, AlGaInAs/InP monolithically integrated DFB laser array, IEEE Journal of Quantum Electronics, 48 (2012) 137–143.
[20] L. Hou, M. Haji, C. Li, B. C. Qiu, and A. C. Bryce, 80-GHz AlGaInAs/InP 1.55 μm colliding-pulse mode-locked laser with low divergence angle and timing jitter, Laser Phys. Lett. 8 (2011) 535–540.
[21] L. Hou, M. Haji, J. Akbar, J. H. Marsh, Narrow linewidth laterally-coupled 1.55μm AlGaInAs_InP DFB laser integrated with a curved tapered SOA, Opt. Lett. 37 (2012) 4525–4527.
[22] L. Hou, M. Haji, J. H. Marsh, A. C. Bryce, 490-fs pulse generation from a passive C-band AlGaInAs/InP mode-locked laser, Opt. Lett. 37 (2012) 773-775.